C. R. Geoscience 351 (2019) 243–252

Contents lists available at ScienceDirect

Comptes Rendus Geoscience

www.sciencedirect.com

Internal Geophysics (Physics of Earth's Interior)

Structural phase transitions in aluminium above 320 GPa

Guillaume Fiquet [a,*], Chandrabhas Narayana [b], Christophe Bellin [a], Abhay Shukla [a], Imène Estève [a], Art L. Ruoff [c], Gaston Garbarino [d], Mohamed Mezouar [d]

[a] IMPMC, Sorbonne Université, UMR CNRS 7590, Muséum national d'histoire naturelle, IRD, 4, place Jussieu, 75252 Paris cedex 05, France
[b] Chemistry and Physics of Materials Unit, Jawaharlal Nehru Centre for Advanced Scientific Research, Jakkur P.O., 560064 Bangalore, India
[c] Materials Science and Engineering, Cornell University, 14853-1501 Ithaca, NY, USA
[d] European Synchrotron Radiation Facility, BP 220, 38043 Grenoble cedex, France

ARTICLE INFO

Article history:
Received 11 May 2018
Accepted after revision 1st August 2018
Available online 28 September 2018

Handled by James Badro

Keywords:
Aluminium
Structural transition
X-ray diffraction
Multi-megabar

ABSTRACT

With the application of pressure, a material decreases in volume as described in its equation of state, which is governed by energy considerations. At extreme pressures, common materials are thus expected to transform into new dense phases with extremely compact atomic arrangements that may also have unusual physical properties. For aluminium, first principle calculations have consistently predicted a phase transition sequence fcc–hcp–bcc in a pressure range below 0.5 TPa [1–7]. The hcp phase was identified at 217 GPa in an experiment (Akahama et al., 2006), and the bcc phase has been recently confirmed in a dynamic ramp-compression experiment coupled with time-resolved X-ray diffraction (Polsin et al. 2017). Here we confirm this observation with a synchrotron-based X-ray diffraction experiment carried out within a diamond-anvil cell and report indications of the onset of the transition towards a bcc structure at pressures beyond 320 GPa. With this work, we also demonstrate the possibility of routine static high-pressure experiments with conventional bevelled diamond-anvil geometry in the 0.3–0.4 TPa regime.

1. Introduction

The extreme pressure phase diagram of materials is important not only for the understanding of the interiors of planets or stars, but also for the fundamental understanding of the relation between the crystal and electronic structures. Structural transitions induced by extreme pressures are governed by the deformation of the charge density of the valence electrons, which bears the brunt of the increasing compression while the relative volume occupied by the nearly incompressible ionic core electrons increases. This fact is said to hold not only in the few hundred GPa range, but also beyond the terapascal regime where compression pushes ion cores together. Experimental limitations will however keep the TPa regime in the realm of predictions, at least as far as static pressure is concerned.

Early first principles calculations (Moriarty and McMahan, 1982) for aluminium (Al) predicted an fcc → hcp → bcc structural transition trend over a pressure range of roughly 0–500 GPa, and these have since been repeatedly confirmed (Boettger and Trickey, 1984; Lam and Cohen, 1983;

* Corresponding author.
E-mail address: guillaume.fiquet@sorbonne-universite.fr (G. Fiquet).

https://doi.org/10.1016/j.crte.2018.08.006

McMahan and Moriarty, 1983) and refined (Boettger and Trickey, 1996; Jona and Marcus, 2006; Sin'ko and Smirnov, 2002). This non-intuitive generic transition from a compact (fcc or hcp) to a more open (bcc) structure with increasing pressure is said to be driven by the increasingly smaller and restricted volume available for the valence electrons. This tends to reduce electronic bandwidth by the occupation of an s–d band at a few hundred GPa (as opposed to the dispersive s–p band at low pressures). Ultimately, theoretical calculations indicate that valence electrons can be localized in "interstitial" spaces in an open-packed incommensurate host-guest structure similar to that predicted at 3.2 TPa (Pickard and Needs, 2010). That d electrons play a role in these transitions is strongly suggested by the fact that the structure sequence with increasing pressure is mirrored in transition metals as the number of d electrons increases (Skriver, 1985) – the analogy has obvious limitations, since the underlying magnetism intervenes in transition metals (Monza et al., 2011). As the unit cell volume is reduced to fractions approaching half or less, the initially unoccupied d bands in simple metals and, in particular, in aluminium approach, narrow, and descend below the Fermi level triggering structural changes which can be intuitively understood since the bcc structure is more compatible with a bonding interaction between second nearest-neighbour atoms than the fcc structure (Moriarty and McMahan, 1982; Lam and Cohen, 1983). Such a transition has earlier been reported in Mg (Olijnyk and Holzapfel, 1985) and Pb (Mao et al., 1990), where it takes place at lower pressures.

A simple system like Al is not only important as a benchmark for theory, but can also be used as a standard for pressures in the TPa range and beyond, which are targeted at dynamic compression facilities such as the National Ignition Facility (NIF) at the Lawrence Livermore National Laboratory in the US or Laser Mégajoule (LMJ) in Bordeaux in France. Confirming predictions of aluminium structure at extremely high densities is thus paramount. According to a recent first principle calculation (Jona and Marcus, 2006), aluminium should undergo a phase transition from fcc to hcp structure around 200 GPa and another transition from hcp–to–bcc with further compression beyond 300 GPa. The hcp phase around 217 GPa was reported in an earlier room-temperature static high-pressure experiment where a maximum pressure of 330 GPa was achieved (Akahama et al., 2006). An earlier classical shock-compression study found no evidence of the predicted fcc–to–hcp transition (Nellis et al., 1988), but it is expected that fcc aluminium melts at 125–150 GPa along principal Hugoniot (see Polsin et al., 2017). More recently, bcc aluminium has been synthesized in the non-equilibrium conditions of an ultra-fast laser-induced micro-explosion confined inside a sapphire (α-Al_2O_3) rod (Vailionis et al., 2011). This recent report of the bcc super-dense phase of Al is interpreted as a complex route of synthesis via a spatial separation of Al and O ions in short-lived hot non-equilibrium plasma of solid-state density. The micro-explosion confined inside a sapphire capsule leads to this bcc-Al phase, which survives in a compressed state after fast quenching. However, if confined micro-explosions provide an interesting route to create and recover high-density polymorphs, such an experiment does not allow the determination of a transition pressure nor does it show any evidence of the presence of a quenched hcp phase. Very recently, an experiment succeeded to combine nanosecond *in situ* X-ray diffraction and simultaneous velocimetry measurements to determine the crystal structure and pressure of ramp-compressed aluminium at stress states between 111 and 475 GPa (Polsin et al., 2017). The solid–solid Al phase transformations, fcc–hcp and hcp–bcc, are reported at 216 ± 9 and 321 ± 12 GPa, respectively. In this article, we confirm this observation with a synchrotron-based X-ray diffraction experiment carried out within a diamond-anvil cell and report indications of the onset of the transition towards a bcc structure at pressures beyond 320 GPa.

2. Experimental

2.1. Sample preparation

Central to our experiment was the establishment of a protocol for reaching pressures exceeding 350 GPa in a diamond-anvil cell with a pure aluminium sample (Fig. 1) confined inside a conventional gasket (Fig. 2), which limits the deviatory stress component to moderate values. Very fine-grained aluminium powder is very difficult to handle and is pyrophoric in nature. It can thus easily oxidize. We used instead an aluminium foil (99.999% purity, 15 μm thickness, Goodfellow) as starting material. Samples were pre-cut from this foil with a focused ion beam (FIB) so as to obtain cylinders (Fig. 1) with dimensions fitting the holes prepared in pre-indented rhenium gaskets.

2.2. Preparation of high-pressure cells and sample loading

Our experiments were conducted in symmetrical diamond-anvil cells equipped with single bevelled diamonds (8° bevel) mounted on X-ray transparent cubic boron nitride seats. Two separate experimental runs were carried out at ambient temperature with diamonds having centre flat culets of 35 and 20 μm diameters, respectively. The first experiment with the 35-μm culet anvil reached 257 GPa, whereas the second one reached pressures of about 370 GPa. In our experiments, no pressure-transmitting medium was used. As noted by Akahama et al. (Akahama et al., 2006), Al has a relatively low shear modulus and is expected to keep low uniaxial stresses in the diamond-anvil cell. The success of experiments in this pressure range is highly dependent on handling samples inside a hole of less than 10 μm, which has to be perfectly centred on a culet of 20 μm made on a gasket pre-indented to less than 10 μm. Manipulating a sample of such small dimensions inside a highly contoured gasket terrain to place it perfectly into the hole is yet another challenge. In the present experiment, we have used the focused ion beam for drilling such tiny holes (see Orloff et al., 2000) in rhenium with a centring precision better than 1 μm and causing very little defects to the gaskets. Rhenium gaskets were pre-indented to reach an initial thickness of about 12 μm, and then drilled with the focused ion beam (FIB).

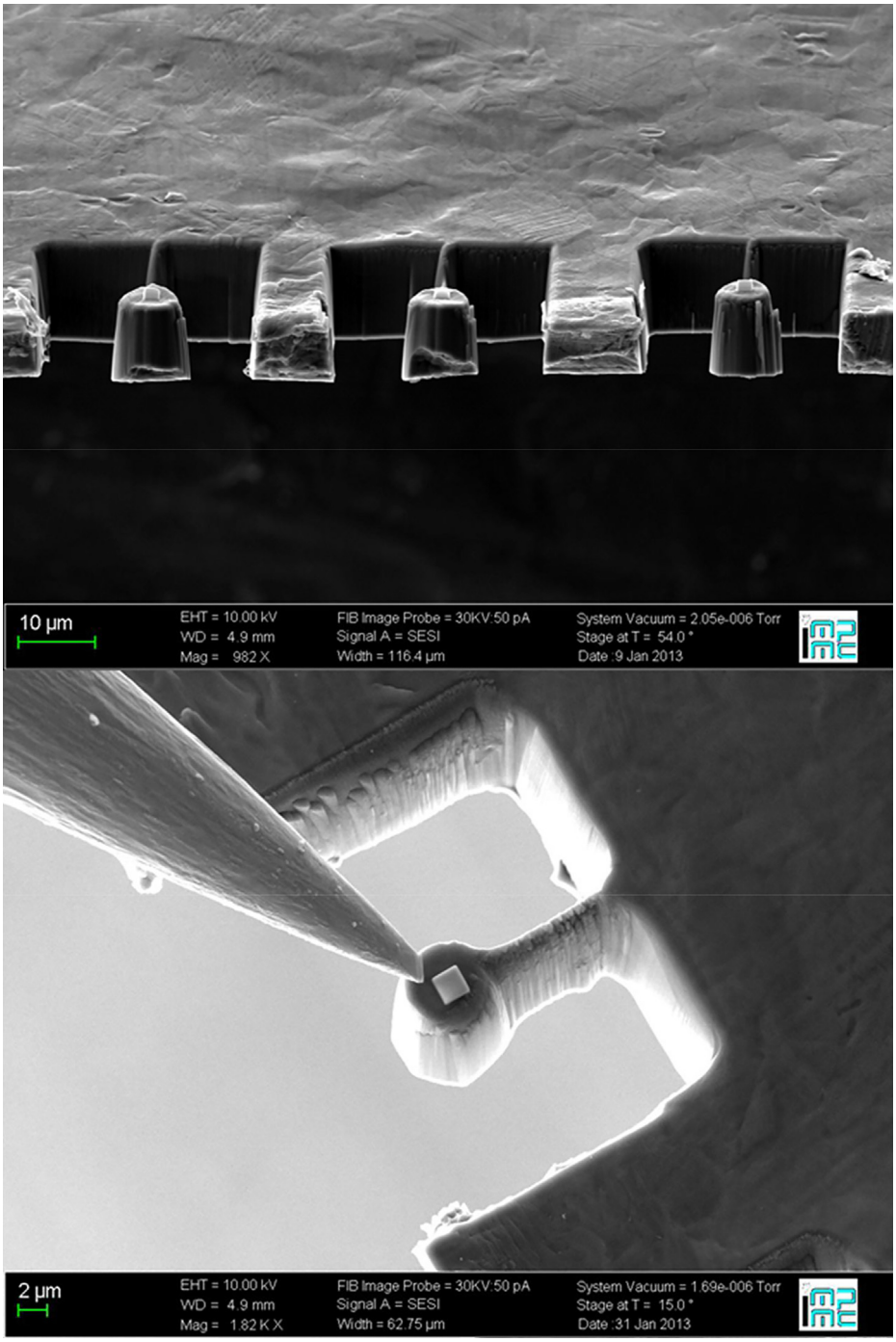

Fig. 1. Secondary electron SEM images: series of sample cylinders shaped with focused ion beam (FIB) on the edge of the pure aluminium sample foil (top). Individual bulk aluminium sample piece during lift-out procedure. The small bridge holding the sample can easily be cut once micro-manipulator is attached. A platinum deposition (2×2 µm light square shape on the top) is visible (bottom). This pressure marker was unfortunately not detected during X-ray diffraction experiments.

Preparation of gaskets and sample loading were carried out in the FIB chamber, so as to have a perfect sample loading in the pressure chambers (see Fig. 2). Above 300 GPa, pressure was estimated according to the equation of state of rhenium (Anzellini et al., 2014). In the fcc stability field, pressure was measured with the available equations of state reported for aluminium (Akahama et al., 2006; Dewaele et al., 2004). Both methods yield pressure measurements in very good agreement (*i.e.* within error bars) up to 300 GPa. Alternatively, the equation of state for rhenium proposed by Dubrovinsky et al., 2012 could be used, but the latter yields significant pressure overesti-

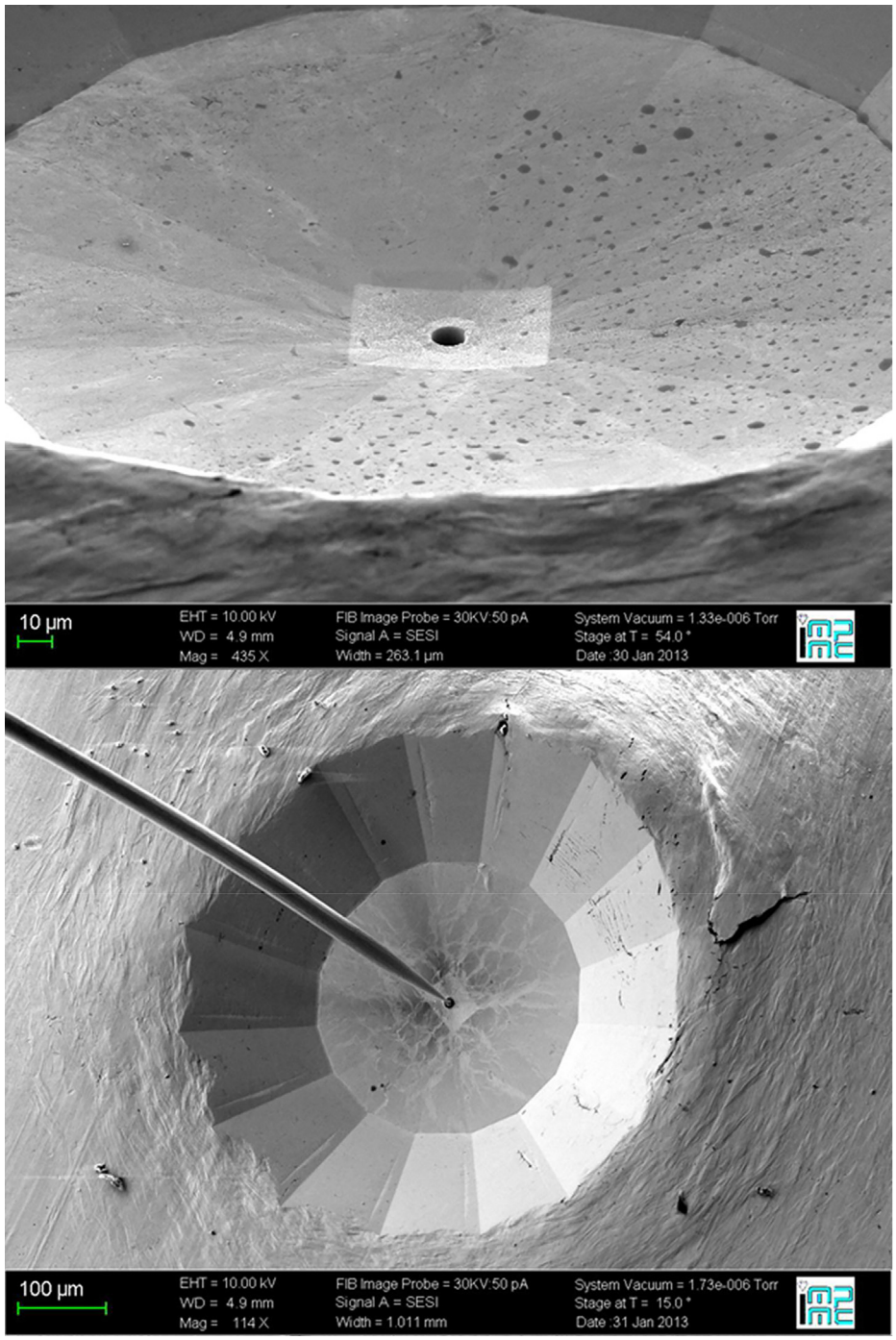

Fig. 2. Secondary electron SEM images: 10-µm hole drilled with FIB at the centre of the 20-µm inner culet print on the rhenium gasket. Outer culet is 300 µm in diameter (top). Sample cylinder loaded with micro-manipulator in sample chamber (bottom).

mate when compared to other measurements (as large as 70 GPa at 300 GPa).

2.3. X-ray diffraction experiments

In situ X-ray diffraction high-pressure experiments were conducted at the high-pressure beamline ID27 of the European Synchrotron Radiation Facility (ESRF, Grenoble, France). X-ray diffraction pattern were collected using an angle-dispersive monochromatic set-up with a wavelength of 0.3738 Å (iodine K-edge at 33.3 keV) focused with KB mirrors down to a spot of 2.5 × 3 µm FWHM at the sample location. Such a spot size explains why rhenium diffraction lines are completely absent in the first run

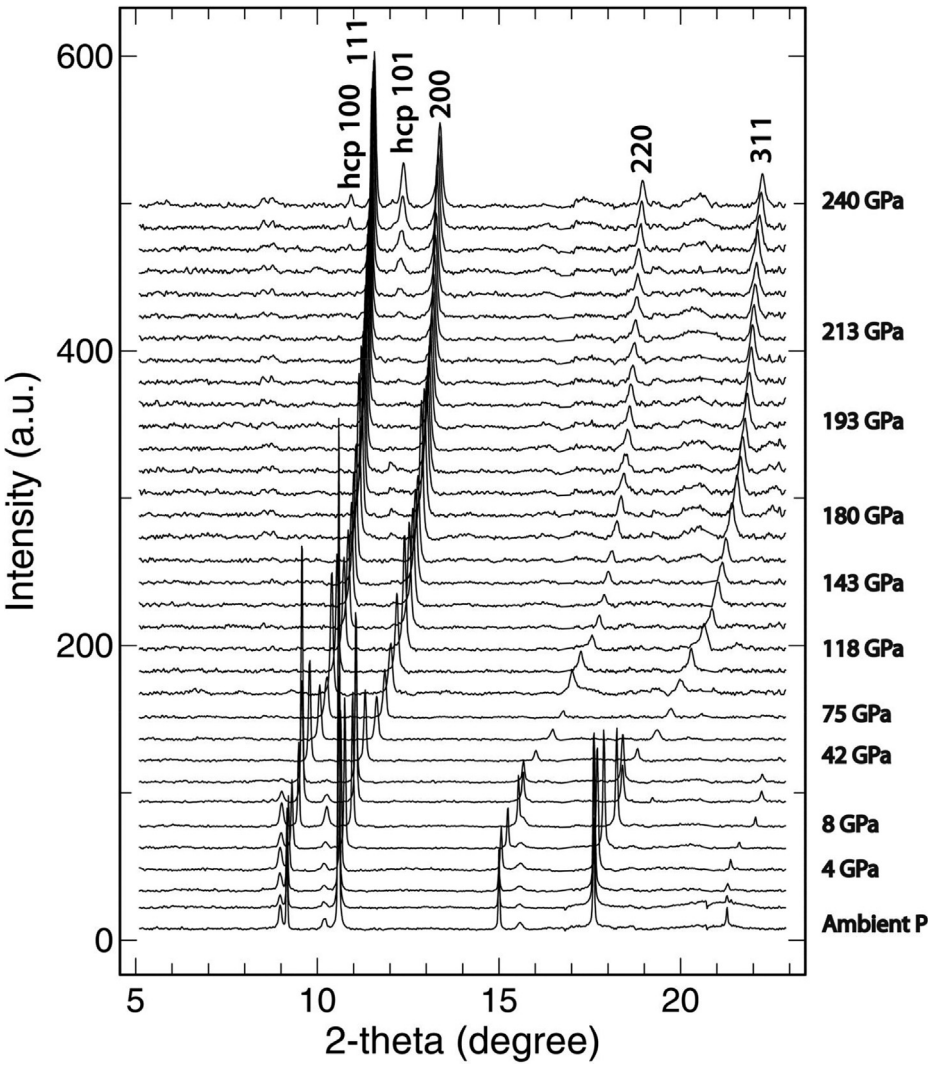

Fig. 3. Diffraction pattern of an fcc aluminium sample compressed in a rhenium gasket at room temperature to 256 GPa in a diamond-anvil cell. Reflections corresponding to the hcp structure are detected at 213 GPa and pressures above.

conducted with bevelled diamonds with a central culet of 35 μm in diameter and a sample chamber of 14 μm in diameter which reached a pressure of 240 GPa (see Fig. 3). Rhenium lines are visible in the second run designed to reach a higher pressure (Fig. 5) with a smaller sample having a diameter of about 8 μm mounted on 20 μm culets. Exposure time varied from 60 s below 100 GPa to 240 s at pressures exceeding 370 GPa, thus compensating for the thickness reduction as pressure was increased. We used a two-dimensional MAR CCD detector located at a distance of 207 mm from the sample. Images were then integrated using the Fit2D software (Hammersley et al., 1996) in order to obtain a conventional diffraction pattern. Data analysis was then carried out using the GSAS package (Larson and Von Dreele, 2000; Toby, 2001). Cell parameters were refined using LeBail method for the extraction of reflection intensity. Preferred orientations were not refined. Graphics were realized with the Datlab software (courtesy K. Syassen, MPI Stuttgart). All X-ray diffraction patterns are background subtracted.

3. Results and discussion

3.1. X-ray pattern analysis

The first run presented in Fig. 3 shows a smooth evolution of the fcc structure at lower pressures. The pattern at 213 GPa can be unambiguously assigned to a fcc lattice with a lattice parameter $a = 3.246$ (1) Å and a unit cell volume of 34.190 (31) Å^3. With four atoms per unit cell in the fcc structure, the atomic volume is 8.548 Å^3. As pressure was increased, new peaks appeared around 220 ± 5 GPa. At the pressure of 235 GPa, as shown in Fig. 4, these new lines can be unambiguously assigned to a hcp structure with lattice parameters $a = 2.266$ (1) Å and $c = 3.720$ (2) Å and a unit cell volume of 16.542 (23) Å^3, coexisting with an fcc lattice with $a = 3.211$ (1) Å and a unit

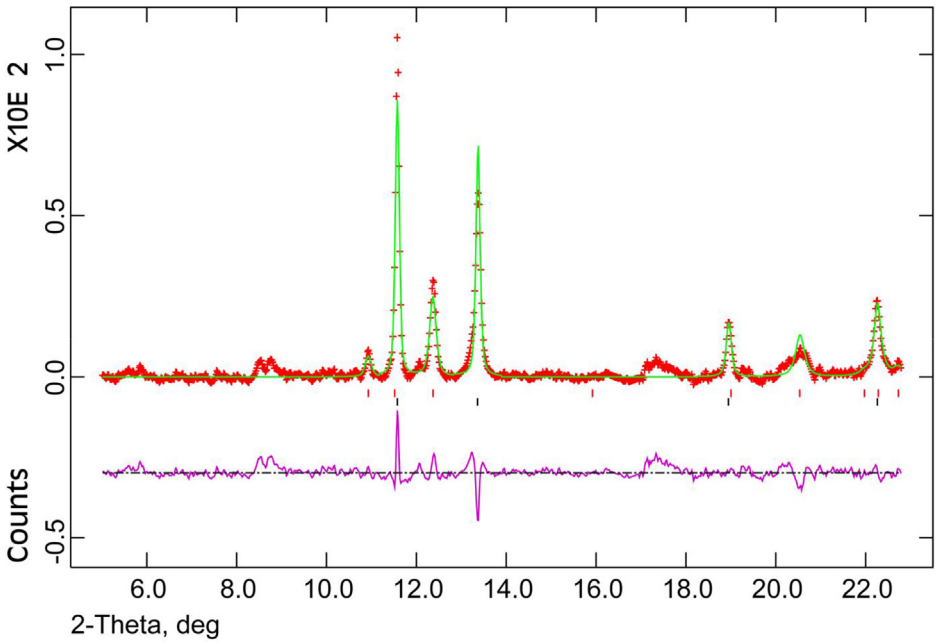

Fig. 4. Analysis of X-ray diffraction pattern of aluminium collected at a pressure of 235 GPa, showing coexisting fcc and hcp structures. The cell parameters are $a = 3.211$ (1) Å and the volume is $V = 33.097$ (30) Å^3 for the fcc phase. The cell parameters are $a = 2.266$ (1) Å and $c = 3.720$ (2) Å with volume $V = 16.539$ (23) Å^3 for the hcp phase.

cell volume of 33.097 (30) Å^3. We find, within error, a similar atomic volume, $V_A = 8.274$ (7) Å^3 for the fcc structure and $V_A = 8.269$ (11) Å^3 for the hcp structure and a large coexistence domain that can be explained by the small enthalpy difference between the two phases (Akahama et al., 2006; Jona and Marcus, 2006; Sin'ko and Smirnov, 2002). These observations are in perfect agreement with the transition pressure of 215–222 GPa reported in the previous X-ray diffraction work cited above (Akahama et al., 2006) or in the dynamic compression experiment (Polsin et al., 2017). Alternatively, a slightly lower pressure of 210 GPa is obtained when using another room temperature high-pressure equation of state for aluminium (Dewaele et al., 2004). This fcc-to- hcp transition takes place at a compression of 0.5, in general agreement with theoretical predictions (*e.g.*, Jona and Marcus, 2006) or experimental measurements (Akahama et al., 2006).

In the second run, we explored pressures above 300 GPa. Patterns are cut at a maximum angle of 20 degrees 2-theta because of the use of higher diamonds. With such a configuration, diamond seats and cell mechanical opening prevented us from collecting diffraction data at higher angles. In this second run (see Fig. 5), we also observe without ambiguity the progressive growth of the hcp phase at the expense of the fcc phase, with the complete disappearance of the fcc peaks at a pressure that can be estimated at about 280 GPa according to the equation of state of aluminium (Dewaele et al., 2004) or that of rhenium (Anzellini et al., 2014). In this run, the presence of rhenium reflections could not be avoided with a sample chamber typically smaller than 8 μm as soon as pressure has been increased. At 235 GPa, lattice parameters $a = 2.266$ (1) Å and $c = 3.720$ (2) Å for the hcp structure yield a c/a ratio of 1.642 (Lam and Cohen, 1983). At 370 GPa, with $a = 2.182$ (2) Å and $c = 3.557$ (5), the c/a ratio is 1.630 (Boettger and Trickey, 1984). It thus seems that the trend followed by the c/a ratio is a decrease when pressure is increased. Between 320 GPa and 350 GPa, the most interesting feature is the observation of a splitting of the 002 reflection of the *hcp* structure (see Fig. 6). The remaining peaks corresponding to the *hcp* structure (100 and 101) do not show any significant broadening nor splitting. It is indeed shown in Figs. 6B and 6C that a new line here interpreted as the 110 bcc grows as a shoulder of the hcp 002 line. Some diffracted intensity detected around a 2-theta value of 17° close to that of the aluminium 102 hcp reflection (see Fig. 5) can tentatively be interpreted as the 200 bcc reflection.

4. Discussion

The hcp ↔ bcc transformations with pressure are martensitic transitions that result from small relative movements of atoms. The hcp → bcc transition has been studied in some detail from the theoretical point of view for the case of Mg (Wentzcovitch, 1994; Wentzcovitch and Cohen, 1988). It is thought to involve a distortion of the regular hexagonal atomic arrangement in the (001) hcp plane as well as a shear between adjacent (001) planes (see Fig. 7). The distortion accounts for the transformation of the (001) hcp planes into the (110) bcc planes, while the shear transforms the ABAB stacking along the [001] hcp direction to one compatible with the bcc structure. This mechanism principally involves the (001) hcp planes and would thus manifest itself by changes in peaks with 00l hcp character. This is exactly what we observe in our experiments as shown in Fig. 6 with a clear splitting of the 002 hcp line when pressure exceeds 320 GPa. It is expected

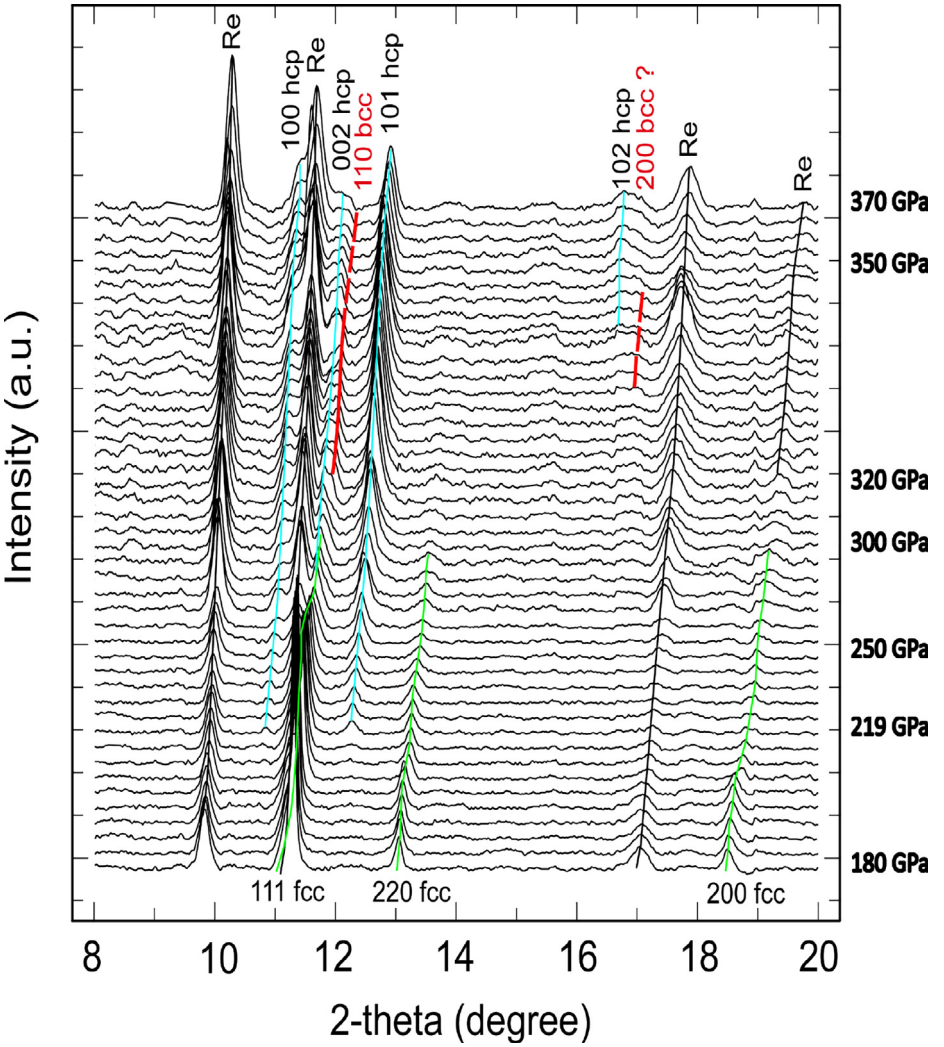

Fig. 5. Series of full diffraction patterns collected between 180 to 370 GPa from the bottom to the top of the figure. The green (fcc), blue (hcp), and red lines (bcc) are guide to the eye for the different aluminium phases. The fcc phase is no longer observed at pressures exceeding 280 GPa. With the reduced size of the rhenium gasket pressure chamber, rhenium diffraction lines cannot be avoided at these pressures.

the 002 hcp reflection should totally disappear with the appearance of a single 110 bcc peak when the transition is completed. However, it is likely the martensitic nature of such a transition that makes the phase transition sluggish at ambient temperature where the transformation is kinetically inhibited, as observed in other systems at room temperature (see (Cynn et al., 2001)). Both low-pressure and high-pressure structures coexist on a large pressure domain and hcp reflections can still be observed at the pressure of 370 GPa as shown in Figs. 5 and 6, although the bcc features are less marked at this maximum pressure because of a diminution of the quality of our diffraction images. Though, our observations are compatible with the observations reported in the ramp-compressed aluminium experiment (Polsin et al., 2017) where the coexistence of the two high-pressure structures is no longer observed above 380 GPa. It is however likely that kinetic barriers can be more easily overcome in shock experiments, whereas it was impossible to heat up our sample kept under such pressure conditions in our experiment. We propose therefore that the peak splitting observed above 320 GPa corresponds to the onset of the hcp–to–bcc structure transition, with compression along the [001] axis. In a rigid atom model, the bcc → hcp transition can be explained simply by using the relationships between the atomic radius r and the lattice parameters a_0 and c_0, with $a_0 = 2r$, $c_0 \approx 1.633\, a_0$ for a hcp structure and $a_0 = 4r/\sqrt{3}$ for a bcc structure, since the atomic packing fraction is higher in the hcp phase. In addition, the relations $a_{hcp} = \sqrt{3}\, a_{bcc}/2$ and $c_{hcp} = \sqrt{2}\, a_{bcc}$ can also be written for such a transition (see Yao and Klug, 2012, for instance), and the cell parameters that we could deduce from our experiments satisfy these relations. In our experiment, the unit cell volume fitted for the hcp structure at 320 GPa is $V_{hcp} = 15.655\ (41)$ Å^3, while that calculated assuming that the split peak corresponds to 002 bcc yields $V_{bcc} = 15.719\ (56)$, which are indiscernible within error bars at the onset of the transition. The observed pattern and reflections are shown for the two

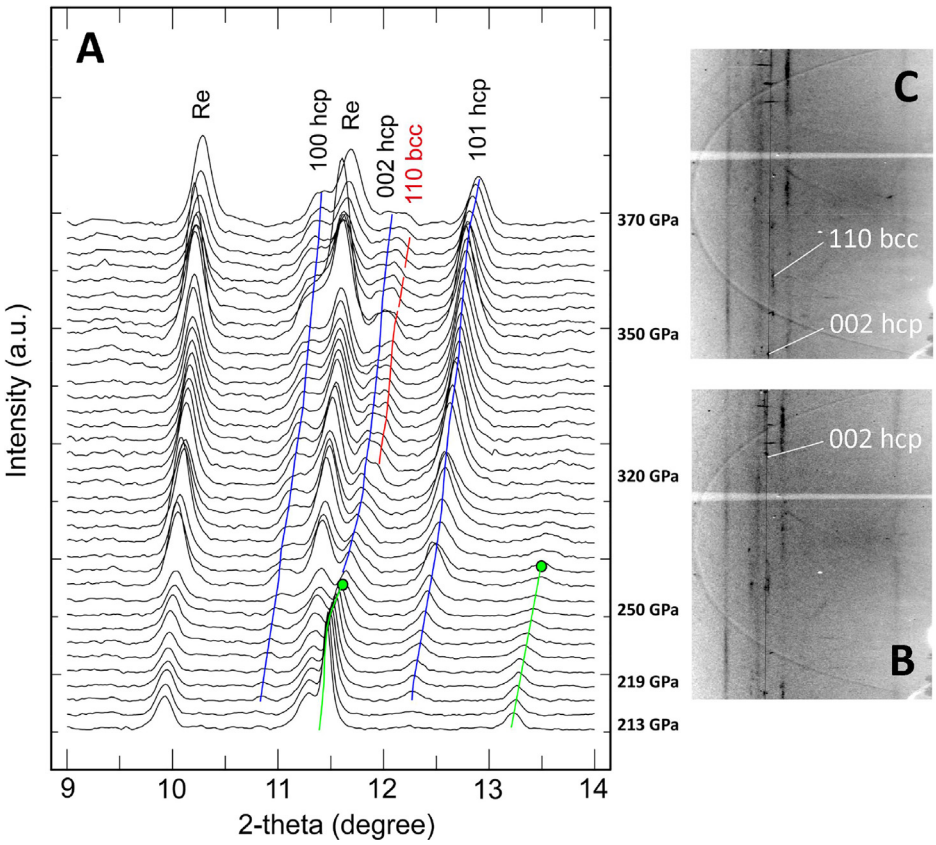

Fig. 6. (A) Detailed view of the peak splitting observed at pressures above 320 GPa. Pattern collected between 280 to 370 GPa from bottom to top of the figure. Blue lines (hcp) and red lines (bcc) are guide to the eye for the different aluminium phases. (B) Cake image of the pattern recorded at 310 GPa, showing hcp 002 spotty reflections (C) Cake image of the pattern recorded at 330 GPa, showing the splitting of hcp 002 and bcc 110 reflections. A thin black line serves as a reference guide for the 002 hcp reflection.

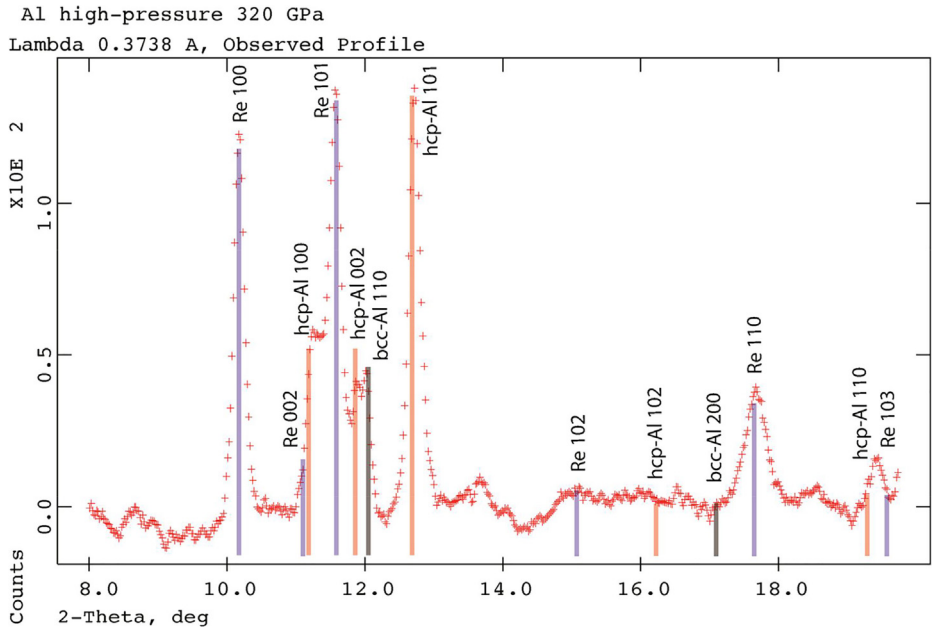

Fig. 7. Observed diffraction at 320 GPa at the onset of the hcp–bcc transition. Fitted cell parameters are $a = 2.230$ (2) Å and $c = 3.635$ (3) Å for a unit cell volume of 15.655 (41) $Å^3$ for the hcp structure, coexisting with a bcc lattice with $a = 2.505$ (3) Å and a unit cell volume of 15.719 (56) $Å^3$.

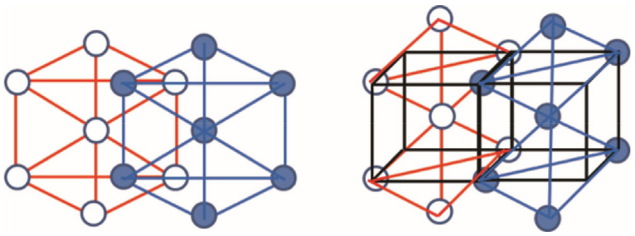

Fig. 8. Left panel: view of adjacent (001) planes with ABAB stacking in the hcp structure, seen along the [001] axis. Right panel: view of adjacent (110) planes in the bcc structure derived from the (001) hcp planes by distortion and shear, with underlying bcc unit cells.

phases at 320 GPa in Fig. 7. At this pressure, the aluminium *d*-spacing for the bcc 110 reflection is 1.771, which is comparable to values reported at the same pressure in Polsin et al., 2017.

We note that the transition to the bcc phase is predicted in the region between 290 and 310 GPa (Sin'ko and Smirnov, 2002) or around 380 GPa (Tambe et al., 2008) by first principles calculations, which respectively account for zero-point thermal vibrations or neglect these. These pressures compare well with the onset of the transition, which we place at 320 GPa. We also have a perfect agreement with the 321 ± 12 GPa measured by velocimetry in the dynamic compression experiments (Polsin et al., 2017). According to theoretical studies, the calculated enthalpy difference between these phases is only a few mRy (Olijnyk and Holzapfel, 1985; Jona and Marcus, 2006; Sin'ko and Smirnov, 2002), and one would experimentally expect these phases to co-exist over a large pressure range as in the case of the fcc–to–hcp transition. We can thus anticipate a very sluggish hcp–to–bcc transition. Our observations correspond to the first step of this transition, built here on a distortion of the hcp lattice (Fig. 8).

Our experiment thus confirms the measured and predicted fcc–hcp–bcc phase transitions for Al. It also supports the predicted mechanism for this martensitic transition via a distortion and shear of the (001) hcp planes. Experiments permitting higher pressures than those reached here will be needed to detect a pure bcc phase unequivocally. Though a recent static pressure experiment has reached a pressure exceeding 1 TPa (Dubrovinskaia et al., 2016), our experiment, performed on a sample of physical interest in conventional static pressure geometry, still opens new perspectives. It provides a large pressure window (up to 4 Mbar) for the study of a wide variety of materials and phenomena in conventional diamond-anvil cell geometry. These range from structural phase transitions or the detection of novel physical properties (such as superconductivity) in elemental or more complicated materials of physical or geophysical interest (Narayana et al., 1998; Zha et al., 2012).

Acknowledgements

The focused ion beam (FIB) and scanning electron microscopy (SEM) facility of the "Institut de minéralogie, de physique des matériaux et de cosmochimie" is supported by the "Région Île-de-France" grant SESAME 2006 No. I-07-593/R, INSU–CNRS, INP–CNRS, Université Pierre-et-Marie-Curie–Paris 6, and by the French National Research Agency (ANR) grant ANR-07-BLAN-0124-01. G. Fiquet acknowledges the program MATISSE that contributed to the visit of Pr. Narayana at IMPMC–Sorbonne Université. MATISSE is a Cluster of Excellence led by "Sorbonne Universités" and managed by ANR within the "Investissements d'avenir" program under reference ANR-11-IDEX-0004-02.

References

Akahama, Y., Nishimura, M., Kinoshita, K., Kawamura, H., 2006. Evidence of a fcc-hcp Transition in Aluminium at Multimegabar Pressure. Phys. Rev. Lett. 96, 045505.

Anzellini, S., Dewaele, A., Occelli, F., Loubeyre, P., Mezouar, M., 2014. Equation of state of rhenium and application for ultra high pressure calibration. J. Appl. Phys. 115, 043511, http://dx.doi.org/10.1063/1.4863300.

Boettger, J.C., Trickey, S.B., 1984. Total energy and pressure in the Gaussian-orbitals technique. II. Pressure-induced crystallographic phase transition and equilibrium properties of aluminium. Phys. Rev. B 29, 6434.

Boettger, J.C., Trickey, S.B., 1996. High-precision calculation of the equation of state and crystallographic phase stability for aluminium. Phys. Rev. B 53, 3007.

Cynn, H., Yoo, C.S., Baer, B., Iota-Herbei, V., McMahan, A.K., Nicol, M., Carlson, S., 2001. Martensitic fcc-to-hcp Transformation Observed in Xenon at High Pressure. Phys. Rev. Lett. 86, 4552.

Dewaele, A., Loubeyre, A., Mezouar, P.M., 2004. Equations of state of six metals above. Phys. Rev. B 70, 094112.

Dubrovinskaia, N., Dubrovinsky, L., Solopova, N.A., Abakumov, A., Turner, S., Hanfland, M., Bykova, E., Bykov, M., Prescher, C., Prakapenka, V.B., Petitgirard, S., Chuvashova, I., Gasharova, B., Mathis, Y.-L., Ershov, P., Snigireva, I., Snigirev, A., 2016. Terapascal static pressure generation with ultrahigh yield strength nanodiamond. Sci. Adv. 2, e1600341.

Dubrovinsky, L., Dubrovinskaia, N., Prakapenka, V.B., Abakumov, A.M., 2012. Implementation of micro-ball nanodiamond anvils for high-pressure studies above 6 Mbar. Nat. Commun. 3, 1163, http://dx.doi.org/10.1038/ncomms2160.

Hammersley, A., Stevenson, S., Hanfland, M., Fitch, A., Häusermann, D., 1996. Two-dimensional detector software: From real detector to idealised image or two-theta scan. High Press. Res. 14, 235.

Jona, F., Marcus, P.M., 2006. Lattice parameters of aluminium in the Mbar range by first-principles. J. Phys. Condens. Matter 18, 10881.

Lam, P.K., Cohen, M.L., 1983. Calculation of high-pressure phases of A1. Phys. Rev. B 26, 5986.

Larson, A.C., Von Dreele, R.B., 2000. GSAS General Structure Analysis System. Los Alamos National Laboratory Report LAUR, 86–748.

Mao, H.K., Wu, Y., Shu, J.F., Hu, J.Z., Hemley, R.J., Cox, D.E., 1990. High-pressure phase transition and equation of state of lead to 238 GPa. Solid State Comm. 74, 1027.

McMahan, A.K., Moriarty, J.A., 1983. Structural phase stability in third-period simple metals. Phys. Rev. B 27, 3235.

Monza, A., Meffre, A., Baudelet, F., Rueff, J.-P., d'Astuto, M., Munsch, P., Huotari, S., Lachaize, S., Chaudret, B., Shukla, A., 2011. Iron Under Pressure: "Kohn Tweezers" and Remnant Magnetism. Phys. Rev. Lett 106, 247201.

Moriarty, J.A., McMahan, A.K., 1982. High-Pressure Structural Phase Transitions in Na, Mg, and Al. Phys. Rev. Lett. 48, 809.

Narayana, C., Luo, H., Orloff, J., Ruoff, A.L., 1998. Solid hydrogen at 342 GPa: no evidence for an alkali metal. Nature 393, 46.

Nellis, W.J., Moriarty, J.A., Mitchell, A.C., Ross, M., Dandrea, R.G., Ashcroft, N.W., Holmes, N.C., Gathers, G.R., 1988. Metals physics at ultrahigh

pressure: Aluminium, copper, and lead as prototypes. Phys. Rev. Lett. 60, 1414.
Olijnyk, H., Holzapfel, W.B., 1985. High-pressure structural phase transition in Mg. Phys. Rev. B 31, 4682.
Orloff, J., Narayana, C., Ruoff, A.L., 2000. Use of focused ion beams for making tiny sample holes in gaskets for diamond anvil cells. Rev. Sci. Instr. 71, 216.
Pickard, C.J., Needs, R.J., 2010. Aluminium: simple metal no more. Nature Mater. 9, 624.
Polsin, D.N., Fratanduono, D.E., Rygg, J.R., Lazicki, A., Smith, R.F., Eggert, J.H., Gregor, M.C., Henderson, B.H., Delettrez, J.A., Kraus, R.G., Celliers, P.M., Coppari, F., Swift, D.C., McCoy, C.A., Seagle, C.T., Davis, J.-P., Burns, S.J., Collins, G.W., Boehly, T.R., 2017. Measurement of Body-Centered-Cubic Aluminium at 475 GPa. Phys. Rev. Lett. 119, 175702.
Sin'ko, G.V., Smirnov, N.A., 2002. *Ab initio* calculations of elastic constants and thermodynamic properties of bcc, fcc, and hcp Al crystals under pressure. J. Phys. Condens. Matter 14, 6989.
Skriver, H.L., 1985. Crystal structure from one-electron theory. Phys. Rev. B 31, 1909.
Tambe, M.J., Bonini, N., Marzari, N., 2008. Bulk aluminium at high pressure: A first-principles study. Phys. Rev. B 77, 172102.
Toby, B.H., 2001. EXPGUI, a graphical user interface for GSAS. J. Appl. Cryst. 34, 210.
Vailionis, A., Gamaly, E.G., Mizeikis, V., Yang, W., Rode, A.V., Juodkazis, S., 2011. Evidence of superdense aluminium synthesized by ultrafast microexplosion. Nat. Commun. 2, 445, http://dx.doi.org/10.1038/nc omms1449.
Wentzcovitch, R.M., 1994. hcp-to-bcc pressure-induced transition in Mg simulated by *ab initio* molecular dynamics. Phys. Rev. B 50, 10358.
Wentzcovitch, R.M., Cohen, M.L., 1988. Theoretical model for the hcp-bcc transition in Mg. Phys. Rev. B 37, 5571.
Yao, Y., Klug, D.D., 2012. Reconstructive structural phase transitions in dense Mg. J. Phys. Condens. Matter 24, 265401.
Zha, C.-S., Liu, Z., Hemley, R.J., 2012. Synchrotron Infrared Measurements of Dense Hydrogen to 360 GPa. Phys. Rev. Lett. 108, 146402.